Analytical Algorithm for Synthesis of Reconfigurable Metagratings

Sreenath Reddy Thummaluru(1), Debdeep Sarkar(1), and Karu P. Esselle(2)
(1) Department of Electrical Communication Engineering, Indian Institute of Science, Bangalore, India
(2) The School of Electrical and Data Engineering, University of Technology, Sydney, NSW 2007, Australia

Abstract

Metagratings are two-dimensional structures that have become more popular in recent days for their highly efficient wavefront manipulation property and low fabrication complexity compared to gradient metasurfaces. This paper presents a new and efficient algorithm to design the electrically reconfigurable metagratings that can achieve any kind of beam-manipulation in both transmission and reflection. The algorithm is explained by allowing four propagating modes, two in transmission and two in reflection for simplicity. Six meta-atoms per macro-period are selected in constructing the metagrating to provide sufficient degrees of freedom for the optimization. The algorithm is tested on different substrates with different field manipulations and achieves high conversion efficiencies. Finally, the capacitively loaded meta-atoms are replaced by varactor diodes to realize the reconfigurable metagrating.

1. Introduction

Until 5G, the wireless environment is fixed by nature, uncontrollable, and involves optimizing the communication endpoints, i.e., transmitter and receiver sections, based on the feedback received from the output section to achieve the desired performance. Whereas, in the upcoming smart radio environment (SRE), the scatterers placed across the channel also send the feedback along with the receiver section. Based on those feedbacks, not only the communication endpoints but also the scatterers are optimized, which ultimately gives control over the wireless environment [1]. Those scatterers are called with unique names, reconfigurable intelligent surfaces (RISs) or intelligent reflecting surfaces (IRSs). RIS is an apt name compared to IRS because the scatterers should also work in transmit mode.

Recent advancements in metasurfaces pave the way for realizing the RISs [2]. Metasurfaces are 2D versions of metamaterials, composed of sub-wavelength elements (called meta-atoms) on a substrate having sub-wavelength thickness. Such ultrathin devices have a high level of control over the impinging electromagnetic wave and can manipulate the beam to achieve anomalous reflection and refraction, beam-steering, beam-splitting, etc. Designing the metasurface has two levels: macroscopic and microscopic [3]. Microscopic level generally involves full-wave simulations to identify the meta-atoms geometries. In complex beam manipulations required in SREs, metasurface often consists of several meta-atoms per macro period. Finding out the geometries of numerous meta-atoms relying on full-wave simulations will become unreasonable. Another major issue with metasurfaces is having low beam-manipulation efficiencies at extreme output angles.

The problems mentioned in the above paragraph regarding metasurfaces, especially when used in constructing RIS, are solved by exploring the metagratings concept [4]. To achieve anomalous refraction or reflection, a single meta-atom per macro period is sufficient in the case of metagrating [5, 6]. A few meta-atoms per macro period are sufficient for complex beam manipulations. Metagratings work on the diffraction principle: efficiently converting the impinging wave into diffracted modes both in reflection and transmission, and then canceling out the unwanted modes to achieve the required field transformations. Designs of single-layered metagratings for anomalous refraction and reflection [5-7], multilayered metagratings for independently controlling amplitude and phase of diffracted modes [8], and reconfigurable metagratings for dynamic beam-steering [9] are available in the literature.

The reconfigurable metagrating design presented in [9] has biasing lines located in a separate plane other than where meta-atoms are located, which may affect the field transformations. Also, the multiple substrate layers and vias used for biasing increase the losses and fabrication complexity. These drawbacks are addressed in this work by a newly developed algorithm that allows the unloaded conducting wires to be used as biasing lines. Thus, the biasing circuitry and meta-atoms are in the same plane, which eases the fabrication and reduces the losses.

2. Design and Algorithm

When the incident electromagnetic (EM) wave hits the metagrating, currents will be induced on the meta-atoms, making them behave like secondary sources, which re-radiates the incident EM wave. The re-radiated power will be coupled to multiple Floquet-Bloch (FB) modes in both transmission and reflection. Depending on the incident angle (θ_{in}) of the EM wave, we can allow the required

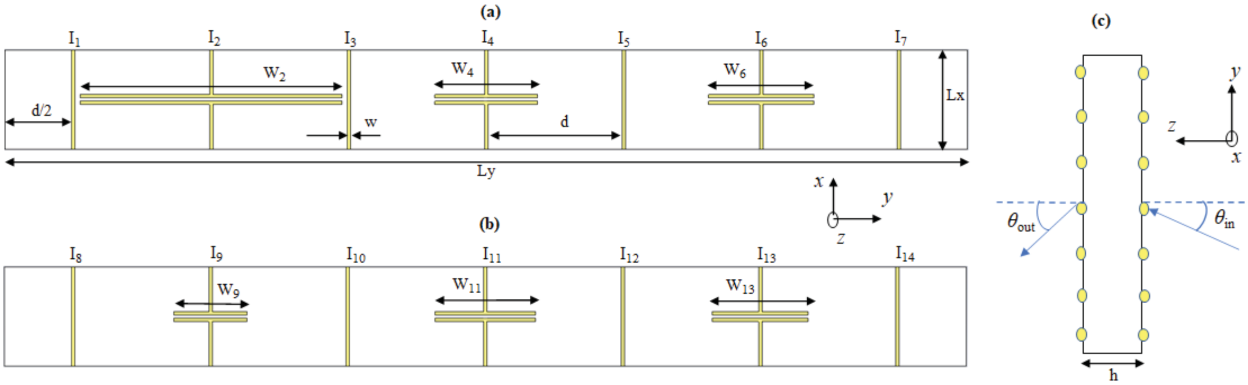

Fig. 1. Metagrating to control four propagating modes. (a) Bottom layer, (b) top layer, and (c) side view showing the incident and outward angles.

Algorithm for designing the reconfigurable metagrating

Input: User will decide the beam-manipulation, substrate on which metagrating to be fabricated, and operation frequency.

Output: The meta-atoms dimensions and their respective capacitances to achieve the desired beam-manipulation.

Step 1: Decide the range of unit cell period (Ly) and incident angle (θ_{in}) for allowing four modes ($m = 0$ and -1 modes), two in transmission and two in reflection.

Step 2: Calculate the allowable range of the outward angle of $m = -1$ mode (i.e., θ_{out}) from Ly and θ_{in} of step 1.

Step 3: Define the complex amplitudes of the four propagating modes based on the desired field manipulation and write them in terms of the induced currents on conducting wires, i.e., $E^T_{-1},\ E^T_0,\ E^R_{-1},\ and\ E^R_0 = f(I_1\ to\ I_{14})$.

Step 4: Find the total field on each individual wire and by using Ohm's law, write the unit length impedances of each wire in terms of the induced currents, i.e., $\tilde{Z}_1\ to\ \tilde{Z}_{14} = f(I_1\ to\ I_{14})$.

Step 5: With matrix inversion, calculate the currents in terms of unit length impedances of the loaded conducting wires (in this problem, six wires are loaded and eight wires are unloaded), i.e., $I_1\ to\ I_{14} = f(\tilde{Z}_2, \tilde{Z}_4, \tilde{Z}_6, \tilde{Z}_9, \tilde{Z}_{11}, \tilde{Z}_{13})$. The impedances of the unloaded conducting wires are zero.

Step 6: Get the amplitudes of propagating modes in terms of the unit length impedances of the loaded conducting wires, i.e., $E^T_{-1},\ E^T_0,\ E^R_{-1},\ and\ E^R_0 = f(\tilde{Z}_2, \tilde{Z}_4, \tilde{Z}_6, \tilde{Z}_9, \tilde{Z}_{11}, \tilde{Z}_{13})$.

Step 7: Identify the impedances of loaded conducting wires by minimizing the function given in Equation (1) and incorporating the non-linear constraints given in Equations (2) and (3). The $\tilde{Z}_{lb}$ and $\tilde{Z}_{ub}$ of Equation (3) depend on the width (W) of the conducting plates of capacitive meta-atoms. The lower boundary of W (which decides $\tilde{Z}_{lb}$) depends on the capability of PCB fabrication machine. The upper boundary of W (which decides $\tilde{Z}_{ub}$) should be less than two times of the separation between the conducting wires.

$$f(\tilde{Z}_2, \tilde{Z}_4, \tilde{Z}_6, \tilde{Z}_9, \tilde{Z}_{11}, \tilde{Z}_{13}) = \sum_{m=-1,0} \left(\eta^R_m - \eta^{target,R}_m\right)^2 + \left(\eta^T_m - \eta^{target,T}_m\right)^2 \qquad (1)$$

$$\text{where } \eta^R_m = \frac{\beta_{m,1}}{\beta_{0,1}}\left|\frac{E^R_m}{E_{in}}\right|^2 \quad and \quad \eta^T_m = \frac{\beta_{m,1}}{\beta_{0,1}}\left|\frac{E^T_m}{E_{in}}\right|^2$$

$$Re(\tilde{Z}_K) = 0 \qquad (2),\ \text{where K} = 2, 4, 6, 9, 11, 13$$

$$Imag(\tilde{Z}_{lb}) < Imag(\tilde{Z}_k) < Imag(\tilde{Z}_{ub}) \qquad (3)$$

Step 8: Finally, calculate the capacitances and their respective widths of meta-atoms by using Equations (4) and (5).

$$C_k = {}^{-1}\!\Big/\!\left(2 \times \pi \times f \times Lx \times Imag(\tilde{Z}_k)\right) \qquad (4) \qquad W_k = {}^{2.85 \times K_{corr} \times C_k}\!\Big/_{\varepsilon_{eff}} \qquad (5)$$

Fig. 2. Algorithm for designing the reconfigurable metagrating having 14 conducting wires and six meta-atoms per unit cell.

modes to propagate and unwanted modes to evanescence by deciding the periodicity of the unit cell (Ly). In this paper, we allowed four modes (m = 0 and −1 modes) to propagate, two in transmission and two in reflection by keeping the periodicity as shown in Eq. (6) [4]. Similarly, there exist some conditions on the outward angle (θ_{out}) because of its relationship with periodicity, as shown in Eq. (7). In general, the distance between the meta-atoms, the substrate's height, and the meta-atoms' dimensions are used as degrees of freedom to achieve the desired field manipulation [4-8]. However, while designing the reconfigurable metagrating, the substrate height and distance between meta-atoms are no more the degrees of freedom; we left with meta-atoms geometries. The minimum number of meta-atoms per unit cell should be greater than or equal to the number of propagating modes to provide sufficient degrees of freedom for the design problem. For more accurate results, this work chooses six meta-atoms per unit cell to control the four propagating modes, as shown in Fig. 1. The conducting wires loaded with meta-atoms are marked by the numbers 2, 4, 6, 9, 11, and 13. The remaining wires are unloaded and act as biasing lines once the meta-atoms are replaced by varactor diodes in the final design. To have a homogeneous current distribution on the wires, the periodicity along the x-axis (Lx) is kept as $\lambda/10$. The distance between any two consecutive wires is kept constant ($d = Ly/7$) in this design, but the user can randomly choose any values. Similarly, it is up to the user to decide his own substrate, i.e., h and ε_r.

$$\frac{\lambda}{1+\sin\theta_{in}} < Ly < \begin{cases} \dfrac{\lambda}{1-\sin\theta_{in}} & 0 < \theta_{in} < \sin^{-1}\left(\dfrac{1}{3}\right) \\ \dfrac{2\lambda}{1+\sin\theta_{in}} & \sin^{-1}\left(\dfrac{1}{3}\right) < \theta_{in} < \dfrac{\pi}{2} \end{cases} \quad (6)$$

$$\sin\theta_{in} - \sin\theta_{out} = \frac{\lambda}{Ly} \quad (7)$$

The algorithm that we developed in designing the reconfigurable metagrating is shown in Fig. 2. As mentioned in step-3 of an algorithm, the complex amplitudes of the four propagating modes can be written in terms of the induced currents on the 14 conducting wires, shown in Eq. (8) and (9). Please see reference [8] to get the knowledge on several unknown parameters mentioned in (8) and (9). For every desired beam manipulation, the induced currents will change accordingly. To get such currents, the metagrating should be loaded with suitable impedances, which can be estimated using Ohm's law, as shown in Eq. (10). The variable K in Eq. (10) is the conducting wires' number, which varies from 1 to 14. The total electric field on each individual wire is composed of the self-induced field because of its own current, external fields, and the coupling fields because of the currents flowing on the other conducting wires. Using matrix inversion, the induced currents can be written in terms of total fields and the load impedances, as mentioned in step-5. Since the impedances of unloaded wires are zero, the currents only depend on the impedances of the loaded wires. Finally, from Eq. (8-10), the complex amplitudes of the four propagating modes can be written in terms of the impedances of the loaded wires, which is nothing but controlling the four modes using six meta-atoms. The loaded impedances can be found by minimizing the Eq. (1) and satisfying the non-linear constraints mentioned in Eq. (2) and (3). For instance, if the desired field manipulation is anomalous reflection, then $\eta_{-1}^{target,R} = 1$, and the remaining three target efficiencies are kept as zero in Eq. (1). Eq. (2) is for minimizing the conductor losses. From the obtained load impedances, one can find their respective capacitances and the conducting plate widths of the capacitive meta-atoms using Eq. (4) and (5). The algorithm is implemented in MATLAB and solved with the help of library functions *fmincon* and *ga*. On some occasions, both the functions have been used, which is nothing but giving the obtained results from *fmincon* to *ga* as inputs. If there is a confusion relating to any parameters used in this paper, we highly recommend you to go through the reference papers [5-9].

$$E_m^R = E_{in}R_{0,1}\delta_{m,0} + \sum_{K=1}^{7} B_{m,1}^{(K)}\, e^{jk_{t,m}d_k} + \sum_{K=8}^{14} B_{m,2}^{(K)}\, e^{jk_{t,m}d_k}\hat{T}_{m,2} \quad (8)$$

$$E_m^T = E_{in}T_{0,1}T_{0,2}\delta_{m,0} + T_{m,2}\sum_{K=1}^{7} A_{m,2}^{(K)}\, e^{jk_{t,m}d_k} + \sum_{K=8}^{14} A_{m,3}^{(K)}\, e^{jk_{t,m}d_k} \quad (9)$$

$$E_K^{total} \text{ at } K\text{th wire location} = \tilde{Z}_K I_K \quad (10)$$

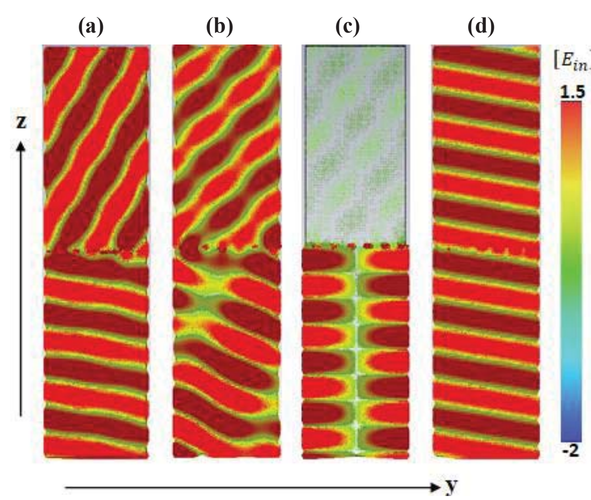

Fig. 3. The E-field distributions of CST for different field manipulations. (a) Anomalous transmission with 98% efficiency having θ_{in} = 10^0 and θ_{out} = -60^0, (b) Beam-splitting in anomalous transmission (48%) and anomalous reflection (47%) having θ_{in} = 18^0 and θ_{out} = -45^0, (c) Specular reflection with 98% having θ_{in} = 10^0 and θ_{out} = -60^0, and (d) Specular transmission with 99% efficiency having θ_{in} = 10^0 and θ_{out} = -60^0

From the obtained meta-atom geometries through MATLAB, the metagrating is constructed in CST software by assigning periodic boundaries and Floquet ports. The E-field distributions of various field manipulations obtained from the CST are shown in Fig. 3. The results shown in Fig. 3 are for the metagrating constructed on Rogers RO3003 substrate at 10 GHz frequency. Once fixing the θ_{in}, θ_{out}, substrate, and operating frequency, the meta-atoms can be replaced by the varactor diodes as shown in Fig. 4, to achieve any kind of beam manipulation. Here, the biasing circuitry is shown only for the bottom layer; similar circuitry can also be used for the top layer. In Fig. 4, two unit cells are considered along x-axis and one unit cell along y-axis. The red and green colored rectangles represent the varactor diodes VD_1, VD_2, and VD_3. The voltages V_1, V_2, and V_3-V_2 are used for controlling VD_1, VD_2, and VD_3, respectively. For every beam-manipulation, the values of loaded capacitances will change, and we achieve those values by controlling the varactor diodes using the biasing voltages. The resistors are placed along the direction perpendicular to the conducting wires, for controlling the current through varactors. Compared to the reconfigurable metagrating presented in [9], the design in this work uses the conducting wires as biasing lines; thus, avoiding the extra substrates and vias for implementing biasing circuitry, which obviously minimizes the losses and reduces the fabrication complexity.

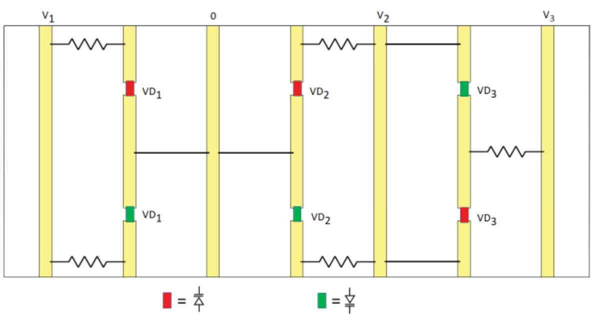

Fig. 4. The possible practical implementation of the reconfigurable metagrating by modifying the configuration of Fig. 1, i.e., replacing meta-atoms with varactor diodes.

3. Conclusion

This paper develops an analytical algorithm to design a reconfigurable metagrating that can achieve the desired field manipulation in both transmission and reflection modes. The algorithm results are tested in a full-wave simulator and obtained high beam manipulation efficiencies. The possible practical implementation of the reconfigurable metagrating is also discussed by giving the biasing circuitry that utilizes the unloaded conducting wires to control the meta-atoms. We believe that this work advances the metagrating field, particularly in smart radio environments involving reconfigurable intelligent surfaces.

References

[1] M. D. Renzo, A. Zappone, M. Debbah, M. -S. Alouini, C. Yuen, J. de Rosny, and S. Tretyakov, "Smart Radio Environments Empowered by Reconfigurable Intelligent Surfaces: How It Works, State of Research, and The Road Ahead," *IEEE Journal of Selected Areas in Communications*, **38**, 11, November 2020, pp. 2450-2525, doi: 10.1109/JSAC.2020.3007211.

[2] M. D. Renzo, M. Debbah, D. -T. Phan-Huy, A. Zappone, M. -S. Alouini, C. Yuen, V. Sciancalepore, G. C. Alexandropoulos, J. Hoydis, H. Gacanin, J. De Rosny, A. Bounceur, G. Lerosey, and M. Fink, "Smart radio environments empowered by reconfigurable AI meta-surfaces: an idea whose time has come," *EURASIP Journal on Wireless Communications and Networking*, **129**, 1, May 2019, pp. 1-20, doi: 10.1186/s13638-019-1438-9.

[3] A. Epstein, and G. V. Eleftheriades, "Huygens' metasurfaces via the equivalence principle: design and applications," *Journal of the Optical Society of America B*, **33**, 2, February 2016, pp. 31-50, doi: 10.1364/JOSAB.33.000A31.

[4] Y. Ra'di, D. L. Sounas, and A. Alù, "Metagratings: Beyond the Limits of Graded Metasurfaces for Wave Front Control," *Physical Review Letters*, **119**, August 2017, p. 067404, doi: 10.1103/PhysRevLett.119.067404.

[5] A. Epstein and O. Rabinovich, "Unveiling the Properties of Metagratings via a Detailed Analytical Model for Synthesis and Analysis," *Physical Review Applied*, **8**, November 2017, p. 054037, doi: 10.1103/PhysRevApplied.8.054037.

[6] O. Rabinovich and A. Epstein, "Analytical Design of Printed Circuit Board (PCB) Metagratings for Perfect Anomalous Reflection," *IEEE Transactions on Antennas and Propagation*, **66**, 8, May 2018, pp. 4086-4095, doi: 10.1109/TAP.2018.2836379.

[7] V. Popov, F. Boust, and S. N. Burokur, "Controlling Diffraction Patterns with Metagratings," *Physical Review Applied*, **10**, July 2018, p. 011002, doi: 10.1103/PhysRevApplied.10.011002.

[8] O. Rabinovich and A. Epstein, "Arbitrary Diffraction Engineering with Multilayered Multielement Metagratings," *IEEE Transactions on Antennas and Propagation*, **68**, 3, March 2020, pp. 1553-1568, doi: 10.1109/TAP.2019.2950813.

[9] A. Casolaro, A. Toscano, A. Alu, and F. Bilotti, "Dynamic Beam Steering with Reconfigurable Metagratings," *IEEE Transactions on Antennas and Propagation*, **68**, 3, March 2020, pp. 1542-1552, doi: 10.1109/TAP.2019.2951492.